STEM CELLS®

CANCER STEM CELLS

Mevalonate Metabolism Regulates Basal Breast Cancer Stem Cells and Is a Potential Therapeutic Target

CHRISTOPHE GINESTIER,[a] FLORENCE MONVILLE,[a] JULIEN WICINSKI,[a] OLIVIER CABAUD,[a] NATHALIE CERVERA,[a] EMMANUELLE JOSSELIN,[a] PASCAL FINETTI,[a] ARNAUD GUILLE,[a] GAELLE LARDERET,[a] PATRICE VIENS,[b,c] SAID SEBTI,[d,e] FRANÇOIS BERTUCCI,[a,b,c] DANIEL BIRNBAUM,[a] EMMANUELLE CHARAFE-JAUFFRET[a,c,f]

[a]Département d'Oncologie Moléculaire, Centre de Recherche en Cancérologie de Marseille, U1068 Inserm, Institut Paoli-Calmettes, Marseille, France; [b]Département d'Oncologie Médicale and [f]Département de BioPathologie, Institut Paoli-Calmettes, Marseille, France; [c]Faculté de Médecine, Université d'Aix-Marseille, Marseille, France; [d]Drug Discovery Department, H. Lee Moffitt Cancer Center and Research Institute, Tampa, Florida, USA; [e]Molecular Medicine Department, University of South Florida, Tampa, Florida, USA

Key Words. Breast cancer • Cancer stem cells • Clinical translation • Gene expression

ABSTRACT

There is increasing evidence that breast tumors are organized in a hierarchy, with a subpopulation of tumorigenic cancer cells, the cancer stem cells (CSCs), which sustain tumor growth. The characterization of protein networks that govern CSC behavior is paramount to design new therapeutic strategies targeting this subpopulation of cells. We have sought to identify specific molecular pathways of CSCs isolated from 13 different breast cancer cell lines of luminal or basal/mesenchymal subtypes. We compared the gene expression profiling of cancer cells grown in adherent conditions to those of matched tumorsphere cultures. No specific pathway was identified to be commonly regulated in luminal tumorspheres, resulting from a minor CSC enrichment in tumorsphere passages from luminal cell lines. However, in basal/mesenchymal tumorspheres, the enzymes of the mevalonate metabolic pathway were overexpressed compared to those in cognate adherent cells. Inhibition of this pathway with hydroxy-3-methylglutaryl CoA reductase blockers resulted in a reduction of breast CSC independent of inhibition of cholesterol biosynthesis and of protein farnesylation. Further modulation of this metabolic pathway demonstrated that protein geranylgeranylation (GG) is critical to breast CSC maintenance. A small molecule inhibitor of the geranylgeranyl transferase I (GGTI) enzyme reduced the breast CSC subpopulation both in vitro and in primary breast cancer xenografts. We found that the GGTI effect on the CSC subpopulation is mediated by inactivation of Ras homolog family member A (RHOA) and increased accumulation of $P27^{kip1}$ in the nucleus. The identification of protein GG as a major contributor to CSC maintenance opens promising perspectives for CSC targeted therapy in basal breast cancer. STEM CELLS *2012;30:1327–1337*

Disclosure of potential conflicts of interest is found at the end of this article.

INTRODUCTION

Breast cancer is a significant health burden and a major therapeutic challenge. The cancer stem cell (CSC) concept provides an attractive oncogenesis model to design new therapeutic strategies able to overcome resistance to conventional therapies and metastatic spread [1]. There is increasing evidence that breast tumors are organized in a hierarchy, with a subpopulation of tumorigenic cancer cells, the CSCs, which sustain tumor growth [2]. Several studies suggest that CSCs resist current anticancer therapies and may induce tumor relapse and recurrence [3]. CSCs are highly invasive and able to generate metastases whereas mature cancer cells are not [4–6]. The characterization of the pathways that regulate CSC biology will allow the targeting of the CSC population, which may significantly improve outcomes for women with breast cancer.

Two main therapeutic approaches have been developed for targeting CSCs [7]. The first approach is based on targeting well-known key pathways regulating CSC survival, differentiation, and self-renewal. Several master pathways

Author contributions: C.G. and E.C.-J.: conception and design, data analysis and interpretation, manuscript writing, and final approval of manuscript; F.M. and N.C.: collection and/or assembly of data and data analysis and interpretation; J.W., O.C., E.J., and G.L.: collection and/or assembly of data; P.F., F.B., and A.G.: data analysis and interpretation; P.V.: administrative support and financial support; S.S.: provision of study material or patients; D.B.: data analysis and interpretation and manuscript writing. C.G. and F.M. contributed equally to this article.

Correspondence: Christophe Ginestier, Ph.D., Department of Molecular Oncology, CRCM, U1068 Inserm, 27 Bd Leï Roure, BP 30059, 13273 Marseille, France. Telephone: 33-(0)4-91-22-35-09; Fax: 33-(0)4-91-22-35-44; e-mail: christophe.ginestier@inserm.fr; or Emmanuelle Charafe-Jauffret, M.D., Ph.D., Department of Molecular Oncology, Institut Paoli Calmettes, 232 Bd. Sainte Marguerite, 13009 Marseille, France. Telephone: 33-(0)4-91-22-35-09; Fax: 33-(0)4-91-22-35-44; e-mail: jauffrete@marseille.fnclcc.fr Received January 23, 2012; accepted for publication April 11, 2012; first published online in STEM CELLS *EXPRESS* May 17, 2012. 1066-5099/2012/$30.00/0 doi: 10.1002/stem.1122

(Hedgehog, NOTCH, and alpha serine/threonine-protein kinase (AKT)/wingless-type MMTV integration site family (WNT)/β-catenin signaling) commonly involved in self-renewal of embryonic and adult stem cells are deregulated in CSCs and induce an expansion of this subpopulation. A number of agents targeting these pathways are currently being tested preclinically, and some have entered clinical trials [3]. The second approach is an unbiased strategy based on the study of CSC-enriched populations using omics technologies or high-throughput screening of small molecule or RNA interference libraries. This second approach allows the identification of new pathways and networks regulating CSC biology. We recently compared the transcriptional profiles of ALDEFLUOR-positive and ALDEFLUOR-negative cells isolated from breast cancer cell lines [4]. We established a gene expression signature that allowed the identification of CXCR1/IL-8 signaling as a key regulatory pathway of breast CSCs. Utilizing a small molecule inhibitor of CXCR1, repertaxin, we were able to specifically target the CSC population in human breast cancer xenografts, delaying tumor growth and reducing metastasis [8].

Breast cancer is a heterogeneous disease that comprises distinct molecular subtypes, including basal, ERBB2, and luminal subtypes. Luminal and basal breast cancers are substantially different at the molecular level [9]. They display different genetic alterations. The cell of origin of the two subtypes may also be different. Recent studies have demonstrated that CSCs may originate from the transformation of normal epithelial cells present at different levels of the hierarchy [10]. CSCs from different breast cancer subtypes may be regulated by different molecular mechanisms. The characterization of basal or luminal CSCs should both provide substantial insight into breast cancer molecular taxonomy and help design new targeted and molecular-focused therapeutic strategies.

In this study, we have sought to identify specific molecular pathways of CSCs isolated from basal or luminal cell lines. Described breast CSC markers ($CD24^-/CD44^+$; ALDEFLUOR-positive) [11, 12] have been useful to isolate CSC in cell lines or primary tumors mainly from the basal or ERBB2 subtypes [4, 13, 14]. The mammosphere assay, based on the unique property of stem/progenitor cells from normal breast to survive and grow in serum-free suspension [15], was also successfully used to establish long-term cultures enriched in CSC from cancer cell lines [16]. The mammospheres formed in these conditions were called tumorspheres. They showed an increase in $CD24^-/CD44^+$ cells and in ALDEFLUOR-positive cells and displayed high tumorigenic potential in non obese diabetes/severe combined immunodeficiency (NOD/SCID) mice [17]. Because the capacity to generate a colony in nonadherent culture conditions is an intrinsic property of immature stem/progenitor cells from all molecular subtypes, the tumorsphere assay might offer the opportunity to screen the CSC regulatory mechanisms either in luminal or in basal subtypes. Here, we have compared the gene expression profiles of cancer cells grown in adherent conditions to matched tumorsphere cultures for five luminal cell lines and eight basal/mesenchymal cell lines. No specific pathway was identified to be commonly regulated in luminal tumorspheres, but enzymes of the mevalonate metabolic pathway were overexpressed in basal/mesenchymal tumorspheres compared to cognate adherent cells. The mevalonate pathway leads to cholesterol synthesis, protein farnesylation, and protein geranylgeranylation (GG). The modulation of this metabolic pathway demonstrated that protein GG is a key factor of breast CSC maintenance. A small molecule inhibitor of the geranylgeranyl transferase (GGTI) reduced the breast CSC population both in vitro and in vivo. We further showed that the GGTI effect on the CSC population was mediated at least in part by the RHOA/$P27^{kip1}$ signaling. This identification of an essential pathway of CSC opens promising perspectives for CSC-targeted therapy in basal breast cancer.

Materials and Methods

Ethics Statement

Use of anonymous human tissue samples was exempted from institutional review board. Animal studies were approved by the Inserm office for Laboratory Animal Medicine.

Cell Lines

A total of 13 breast cell lines (BCL) were obtained either from the American type culture collection (ATCC) (BT-474, BT-483, HCC38, HCC1954, MCF7, MCF10A, SK-BR-7, and T47D; http://www.lgcpromochem-atcc.com) or from collections developed in Dr. S. Ethier's Laboratory (SUM44, SUM149, SUM159, SUM190, and SUM225; http://www.asterand.com). All BCLs tested were derived from carcinomas except MCF10A, which was derived from a fibrocystic disease. The cell lines were grown using the recommended culture conditions [46]. Breast cancer cell lines were treated in adherent conditions with simvastatin (Sigma-S6196; Sigma Aldrich, St Louis, MO, www.sigmaaldrich.com), mevalonate (Sigma-69761), cholesterol (Sigma-C3045), farnesyl transferase inhibitor (FTI-277) (Sigma-F9803), geranylgeranyl transferase inhibitor (GGTI-298) (Sigma-G5169), Rho inhibitor (Cytoskeleton-CT04; Cytoskeleton, Denver, CO, www.cytoskeleton.com), or GGPP (Sigma-G6025).

Anchorage-Independent Culture

BCLs grown in adherent conditions, with or without treatment, were dissociated and plated as single cells in ultra-low attachment plates (Corning, Acton, MA, www.sigmaaldrich.com) at low density (1,000 viable cells per milliliter). Cells were grown as previously described [4]. Subsequent cultures after dissociation of primary tumorspheres were plated on ultra-low attachment plates at a density of 1,000 viable cells per milliliter. The capacity of cells to form tumorspheres after treatment was quantified after the first (primary tumorspheres) and second (secondary tumorspheres) passage.

RNA Extraction

Total adherent cell lines (ADHs) were enzymatically detached with trypsin, dry pelleted, and frozen. Secondary spheres (SPH2) from corresponding ADHs were filtrated, dry pelleted, and frozen. Total RNA was extracted from these pellets using AllPrep DNA/RNA Mini Kit (Qiagen, Hamburg, Germany, www.qiagen.com), following recommended instructions. RNA integrity was controlled by micro-analysis (Agilent, Palo Alto, CA, www.agilent.com).

Gene Expression Profiling

RNA expression profiling was done with Affymetrix U133 Plus 2.0 human oligonucleotide microarrays. Microarrays represented over 47,000 transcripts and variants including 38,500 well-characterized human genes. Preparation of cRNA, hybridizations, washes, and detection were done as recommended by the supplier (Affymetrix, Santa Clara, CA, www.affymetrix.com). Expression data were analyzed by the Robust Multichip Average (RMA) method in R using Bioconductor and associated packages [47, 48], as described [46]. RMA did background adjustment, quantile normalization, and summarization of 11 oligonucleotides per gene. Before analysis, a filtering process removed from the dataset genes with low and poorly measured expression as defined by

expression values inferior to 100 units in the luminal cell line group (five ADH and five SPH2), retaining 20,359 genes/expressed sequence tag (EST) and in the basal cell line group (eight ADH and eight SPH2), retaining 22,354 genes/expressed sequence tag (EST). The molecular subtype of cell lines was defined as previously described [46].

GSEA

Enrichment analysis was done using the GSEA program [18, 48]. The 20,359 probe sets for the luminal cell line group were converted into 11,768 single corresponding genes, and the 22,354 probe sets for the basal cell line group were converted into 12,627 single corresponding genes. First, we applied GSEA to the "mammosphere-derived" gene set [19] containing 185 genes, 92 upregulated and 93 downregulated. Then, we applied GSEA to the C_2-CP functional catalog (curated genes set from online pathway databases, publications in Pubmed, and knowledge of domain experts), containing 439 gene sets representing canonical pathways.

GSMA

We used GSMA for representing GSEA significant pathways. GSMA Z scores were computed for each GSEA significant pathway gene list and for each sample (ADH or SPH2) according to the algorithm first described by Kim and Volsky [49]

$$Z = (Sm - \mu) * m1/2/\sigma,$$

where Sm is the mean of the fold change values of genes contained in significant pathways identified by GSEA and the size of the gene list is m. The mean (μ) and standard deviation (σ) of the total fold change values for a given dataset are calculated for GSEA significant pathways. For each sample (ADH or SPH2), the ratio Z score (sample)/mean Z score (ADH) was calculated and represented by an unsupervised clustering [50] using Pearson correlation and average linkage.

RQ-PCR

mRNA from three different cell lines (ADH and SPH2) were used for RQ-PCR assays in a ABI PRISM 7900HT sequence detection system. Primers and probes for the Taqman system were selected from the Applied Biosystems, Carlsbad, CA, www.appliedbiosystems.com Web site (Hs00926054_m1), Hs00932159_m1), MVK (Hs0017 6077_m1), MVD (Hs00159403_m1), IDI1 (Hs01057440_m1), FDPS (Hs00266635_m1), SQLE (Hs01123768_m1), Hs00158 906_m1), Hs00940273_m1), Hs00999007_m1). The relative expression mRNA level of genes from the mevalonate pathway was computed with respect to internal standards GAPDH and GUSB genes to normalize for variations in the quality of RNA and the amount of input cDNA, as described previously [8].

Cell Viability

For 3-(4,5-dimethylthiazol-2-yl)-2,5-diphenyltetrazolium bromide (MTT) assays, cells were plated in adherent conditions in 96-well plates at 5,000 cells per well. After 1 day, treatment with serial dilutions of selected compounds was started. The effect of treatment on cell viability was estimated after 3 days by addition of 20 μL of MTT solution (5 mg/mL in phosphate buffered saline (PBS)) in each well. Cells were then incubated for 1 hour at 37°C followed by addition of 50 μL of dimethyl sulfoxide (DMSO) to each well. Absorbance was measured at 560 nm in a fluorescence plate reader (Tecan, Mannedorf, Switzerland, www.tecan.com).

Western Blotting

Cells were lysed in extraction buffer (1% (v/v) Triton X-100, 50 mM HEPES, pH 7, 1 mM EDTA, 1 mM EGTA, 150 mM NaCl, 100 mM sodium fluoride, 1 mM Na_3VO_4, and one tablet of CompleteTM inhibitor mix [Roche Applied Science, Indianapolis, IN, www.rocheappliedscience.com] per 25 mL of buffer) and loaded onto SDS-polyacrylamide gels. Blots were incubated with the respective primary antibodies diluted in tris-buffered saline and tween 20 (TBST) (containing 0.1% Tween20 and 2% Milk) and incubated overnight at 4°C. Then, blots were washed and incubated with appropriate secondary antibodies (GE Healthcare, Waukesha, WI, www.gehealthcare.com) and detected using SuperSignal West Pico Chemiluminescent Substrate (Pierce, Rockford, IL, http://www.piercenet.com). Antibodies used for Western blotting were anti-HMGCR (Abcam, Cambridge, UK, www.abcam.com ab99383, 1:200), anti-α-tubulin (Sigma-Aldrich T5168, 1:4,000), anti-FDFT1 (Atlas antibodies, Stockolm, Sweden, www.atlasantibodies.com HPA008874, 1:1,000), anti-pGGT1B (Abcam ab55615, 1:500), anti-Rho A (Santa Cruz Biotechnology, Santa Cruz, CA, www.scbt.com sc-418, 1:500), anti-Rb (Santa-Cruz Sc-102 1:200), and anti-p27Kip1 (Dako, Glostrup, Denmark, www.dako.com, M7203, 1:200).

ALDEFLUOR Assay

The ALDEFLUOR kit (Stemcell Technologies, Vancouver, Canada, www.stemcelltechnologies.com) was used to isolate the population with high aldehyde dehydrogenase (ALDH) enzymatic activity using an LSR2 (Becton Dickinson Biosciences, Sparks, MD, www.bdbiosciences.com) as previously described [12]. In order to eliminate cells of mouse origin from the xenotransplanted tumors, we used staining with an anti-H2Kd antibody (BD Biosciences, 1/200, 20 minutes on ice) followed by staining with a secondary antibody labeled with phycoerythrin (Jackson Labs, Bar Harbor, MN, www.jax.org, 1/250, 20 minutes on ice).

siRNA Lipofection

Three stealth siRNA targeted to the pGGT1B or $p27^{kip1}$ mRNA (Invitrogen, Carlsbad, CA, www.invitrogen.com) were designed along with the corresponding stealth siRNA control. SUM149 cells were lipofected with these four oligonucleotides utilizing lipofectamine RNAiMAX (Invitrogen). A total of 25,000 cells were plated in triplicate in 24-well plates with 10 pmol of siRNA in 600 mL of Opti-MEM I Medium. The ALDEFLUOR-positive population was evaluated in triplicate at 30 hours after lipofection.

Cell Cycle Analysis

Briefly, supernatant and adherent cells were harvested, washed, and suspended in 0.5 mL medium containing propidium iodide (40 mg/mL) and RNase A (40 mg/mL). Analysis of the cell cycle was done on the LSR2 (BD Biosciences) using Diva analysis software.

Animal Models

To explore the efficiency of GGTI treatment on tumor growth, we utilized two primary human breast cancer xenografts generated from two different patients (T226 and T214). GGTI-2418 compound (Tigris Pharmaceuticals/Kirax Corp, Bonita Springs, FL, www.kirax.com) was used for animal experiments. Cells from these tumors were transplanted orthotopically in the humanized cleared fat pad of NOD/SCID mice, without cultivation in vitro. Fat pads were prepared as described previously [12]. We injected 100,000 cells from each xenotransplant in two humanized fat pads of NOD/SCID mice and monitored the tumor growth. When the tumor size was approximately 150 mm^3, we initiated treatment with GGTI-2418 alone (i.p., 100 mg/kg, every day for 14 days), docetaxel alone (i.p., 10 mg/kg, once a week for 2 weeks), in combination (GGTI-2418/docetaxel), or a control group injected with saline (i.p., every day for 14 days). Four mice were injected for each xenotransplant and for each group. The animals were euthanized when the tumors were approximately 500 mm^3, to avoid tumor necrosis

and in compliance with regulations for use of vertebrate animals in research. A portion of each fat pad injected was fixed in formalin and embedded in paraffin for histological analysis. The rest of the tumor cells were analyzed for the ALDEFLUOR phenotype and were reimplantated into secondary NOD/SCID mice, with injection of 5,000 cells for each treated tumor.

Statistical Analysis

Results are presented as the mean ±SD for at least three repeated individual experiments for each group. Statistical analyses used the SPSS software (version 10.0.5). Correlations between sample groups and molecular parameters were calculated with the Fisher's exact test or the one-way ANOVA for independent samples. A p value $<.05$ was considered significant.

Results

Luminal Tumorspheres Are Not Enriched in CSC

We compared gene expression profiles from cell lines cultured in adherent conditions to that of tumorspheres of secondary passage potentially highly enriched in CSCs. Five luminal cell lines (BT-474, BT-483, MCF7, T47D, and SUM44) and eight basal/mesenchymal (HCC38, HCC1954, MCF10A, SK-BR-7, SUM 149, SUM159, SUM190, and SUM225) cell lines were analyzed. To identify the molecular mechanisms that are associated with luminal or basal/mesenchymal breast CSC, we utilized the GSEA (gene set enrichment analysis) algorithm to screen the pathways and gene signatures from the Broad Institute (MSigDB c2: Curated Gene Sets) [18]. Surprisingly, we did not identify any pathway significantly associated with luminal tumorspheres compared to adherent cancer cells (data not shown). A previous study had identified a tumorsphere-derived gene set (Kok gene set) based on the study of four luminal cell lines [19]. The Kok gene set presented mainly a reduction of proliferation and cell cycle-regulated genes in the tumorspheres compared to the adherent cells. Using GSEA, we compared the gene expression profiles of our luminal tumorspheres to this previously described signature. We found a significant enrichment between the Kok gene set and our luminal tumorsphere gene expression profiles (false discovery rate (FDR) <0.01) (Supporting Information Fig. 1). This could be explained by the low proliferation rate of tumor cells in suspension compared to cells cultured in adherent conditions but did not reflect a specific luminal CSC biological feature.

To confirm the absence of specific signaling pathways associated with luminal tumorspheres, we compared the capacity of luminal and basal CSCs to be propagated in suspension in serial tumorsphere passages. We cultured two luminal (MCF7 and T47D) and two basal/mesenchymal (SUM159 and HCC1954) cell lines in suspension and evaluated their tumorsphere formation capacity for five serial passages. Luminal cell lines showed a constant or reduced ability to form tumorspheres in serial passages compared to primary tumorsphere formation (Supporting Information Fig. 2). In contrast, basal/mesenchymal cell lines presented an increase in tumorsphere formation through serial passages ($p < .001$). These results suggest that tumorsphere formation, which is indicative of in vitro CSC self-renewal, is not an appropriate assay to propagate luminal CSCs whereas basal/mesenchymal CSCs are significantly expanded in passaged tumorspheres.

Basal/Mesenchymal Tumorspheres Harbor an Overexpression of Enzymes Involved in the Mevalonate Metabolic Pathways

Gene expression analysis revealed six gene sets significantly associated with basal/mesenchymal tumorspheres compared to adherent cancer cells (enrichment score (ES) >0.8; FDR <0.05). The results are represented using GSMA (gene set matrix analysis), which allows the visualization of enrichment within and between samples by clustering gene sets [20] (Fig. 1A). All the gene sets identified were highly enriched in genes coding for enzymes involved in mevalonic acid (MVA) metabolism. This metabolic pathway (Fig. 1B), which starts by the conversion of 3-hydroxy-3-methylglutaryl CoA (HMG-CoA) to mevalonate through HMG-CoA reductase (HMGCR) activity, allows the production of isoprenoids used for many important physiological processes including cholesterol biosynthesis and protein prenylation (farnesylation and GG) [21]. These lipid post-translational modifications allow proper cellular localization, which regulates the function of these proteins. All the enzymes involved in key steps of MVA metabolism were significantly enriched in basal/mesenchymal tumorspheres with 87% (13/15) and 71% (10/14) of genes regrouped in the "Biosynthesis of Steroids" and "Cholesterol Biosynthesis" gene sets, respectively (Fig. 1A).

We confirmed in separate real-time quantitative PCR (RQ-PCR) analysis that the expression of the genes involved in MVA metabolism was markedly increased in tumorspheres (Fig. 1C; Supporting Information Fig. 3). Finally, we selected two key enzymes (HMGCR and farnesyl-diphosphate farnesyltransferase 1 (FDFT1)) of MVA metabolism for measurement of protein expression by Western blot in three basal/mesenchymal cell lines (Fig. 1D). HMGCR protein expression was detectable in tumorsphere samples but not in cells cultured in adherent conditions. Similarly, FDFT1 protein expression was highly enriched in tumorsphere samples compared to adherent cancer cells. These data suggest that MVA metabolism may be overactivated in basal/mesenchymal tumorspheres and may play an important role in basal/mesenchymal breast CSC biology.

MVA Pathway Blockade Reduces the Basal/Mesenchymal Breast CSC Population In Vitro

To validate the role of MVA metabolism in the regulation of breast CSC biology, we used Simvastatin, an inhibitor of HMGCR, which blocks the biosynthesis of MVA (Fig. 1B). Three basal/mesenchymal cell lines (SUM149, SUM159, and HCC1954) were treated with Simvastatin in adherent conditions with their respective IC50 determined after 3 days of treatment (Supporting Information Fig. 4). The effect of Simvastatin treatment on the CSC population was measured by both the ALDEFLUOR assay and the tumorsphere formation assay. In these cell lines, the ALDEFLUOR-positive population contains the CSC population [4]. Simvastatin treatment reduced the CSC population, with three times less ALDEFLUOR-positive cells after 3 days of treatment (Fig. 2A, 2B; Supporting Information Fig. 5). Similarly, Simvastatin-treated cells cultured in tumorsphere conditions formed six times fewer primary and secondary tumorspheres than in the control (Fig. 2C, 2D; Supporting Information Fig. 6). The addition of mevalonate, the product of HMGCR, to the culture medium, rescued the CSC population, with a complete restoration of both the ALDEFLUOR-positive population and the tumorsphere-initiating ability (Fig. 2A–2D; Supporting Information Figs. 5A, 6). These results confirm the essential role of MVA metabolism in the regulation of CSC self-renewal.

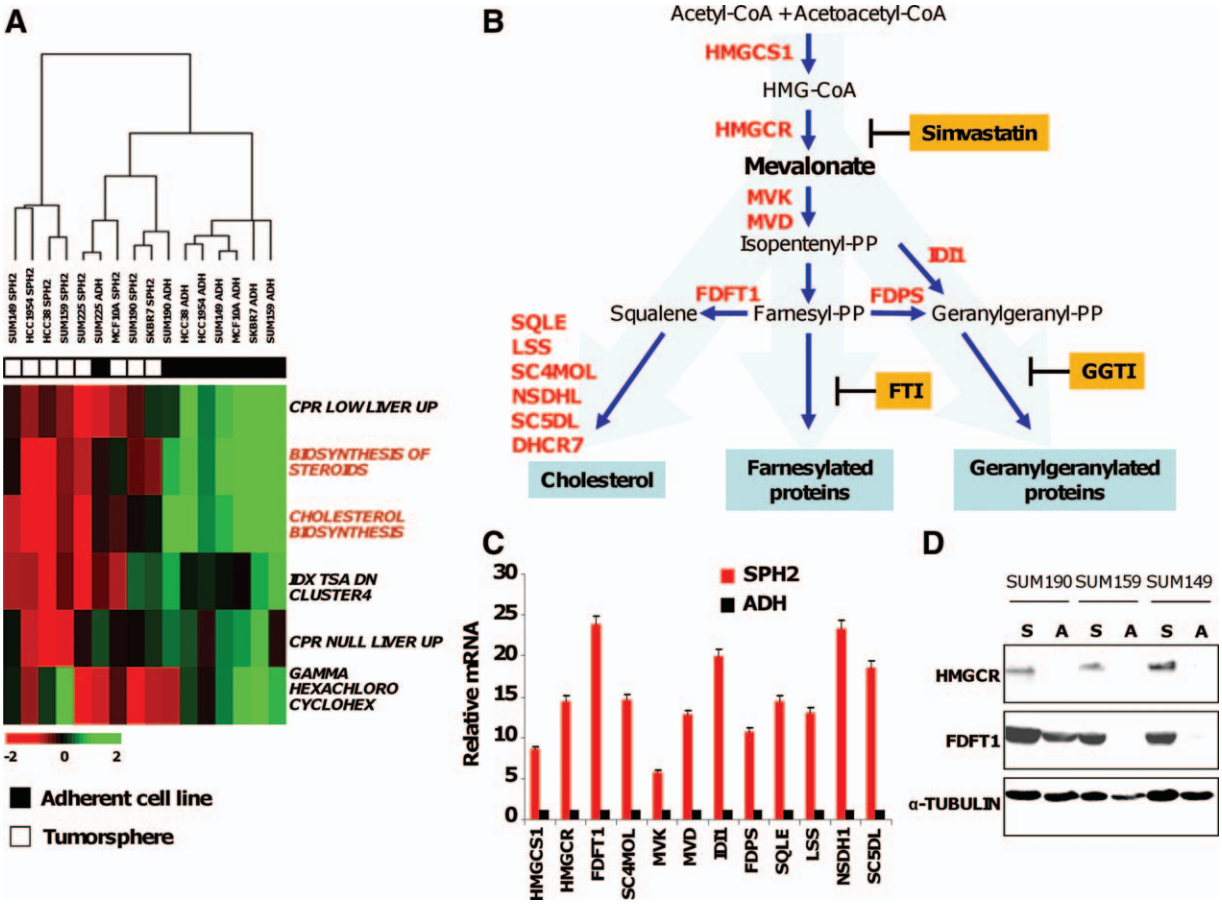

Figure 1. Basal tumorspheres overexpress genes involved in mevalonic acid (MVA) metabolism. (**A**): Gene expression profiles from eight basal cell lines cultured in adherent conditions compared to cells cultured for tumorspheres to secondary passage. Results are represented using gene set matrix analysis. Gene sets significantly associated with tumorspheres are represented on hierarchical clustering. This gene set list is enriched in pathways involved in MVA metabolism (gene sets in red). (**B**): Schematic diagram of the MVA metabolism. Genes significantly overexpressed in tumorspheres and coding for enzymes involved in MVA metabolism are represented at their respective sites of action (in red). Similarly, the site of action of compounds used to inhibit MVA metabolism are represented (orange box). (**C**): We measured the level of mRNA, by real-time quantitative PCR, for 12 different genes involved in MVA metabolism and confirmed the increase of MVA metabolism's genes in tumorspheres compared to adherent cells (Fisher test; $p < .001$). Similar results were observed for SUM159 cell line and HCC1954 (Supporting Information Fig. 3) (**D**): Analysis of HMGCR and FDFT1 protein expression by immunoblotting in adherent cells compared to tumorspheres. These two key enzymes of MVA metabolism were significantly overexpressed in tumorspheres. A (or ADH) and S (or SPH2) designate adherent and tumorsphere, respectively. Abbreviations: ADH, adherent cell line; FDFTI, farnesyl-diphosphate farnesyltransferase 1; GGTI, geranylgeranyl transferase I; HMG-COA, hydroxy-3-methylglutaryl CoA; HMGCR, HMG-CoA reductase; SPH2, secondary spheres.

Simvastatin Effect on CSC Population Is Not Mediated Through Cholesterol Biosynthesis Blockade or Protein Farnesylation Inhibition. Because MVA metabolism generates several endproducts (cholesterol, isoprenoids), we sought to identify the downstream limbs of the mevalonate metabolic pathway involved in CSC regulation. We first examined the compensatory effect of exogenous cholesterol on Simvastatin treatment. Addition of cholesterol did not prevent Simvastatin effect on CSC population with a similar reduction in the ALDEFLUOR-positive population and tumorsphere-initiating capacity in all three cell lines analyzed (Fig. 2A–2D; Supporting Information Figs. 5A, 6). Second, we examined the effect of protein farnesylation inhibition on the CSC population. We treated cells with the farnesyl transferase inhibitor FTI-277 (FTI) that inhibits protein farnesylation (Fig. 1B). After 3 days of FTI treatment (Supporting Information Fig. 4), we did not observe any effect on the ALDEFLUOR-positive population or on the tumorsphere formation for all three cell lines analyzed (Fig. 2A–2C; Supporting Information Figs. 5B, 6).

These results suggest that the ability to affect the breast CSC population via MVA metabolism blockade is neither related to cholesterol biosynthesis nor to protein farnesylation.

Protein GG Inhibition Recapitulates Simvastatin Treatment Effect on the Breast CSC Population

To explore whether protein GG is preferentially involved in CSC regulation, we treated three cell lines with GGTI-specific inhibitor GGTI-288 (GGTI) and performed the CSC assays. Cells were treated in adherent conditions with their respective IC50 determined after 3 days of GGTI treatment (Supporting Information Fig. 4). We observed that protein GG inhibition strongly reduced the CSC population with less than 0.3% of residual ALDEFLUOR-positive cells in the GGTI-treated cell population (Fig. 3A; Supporting Information Fig. 5B). Similarly, GGTI reduced the ability to generate primary and secondary tumorspheres in treated cells (Fig. 3B; Supporting Information Fig. 6). To further prove that the effect of MVA blockade on the CSC population is exclusively due to GG

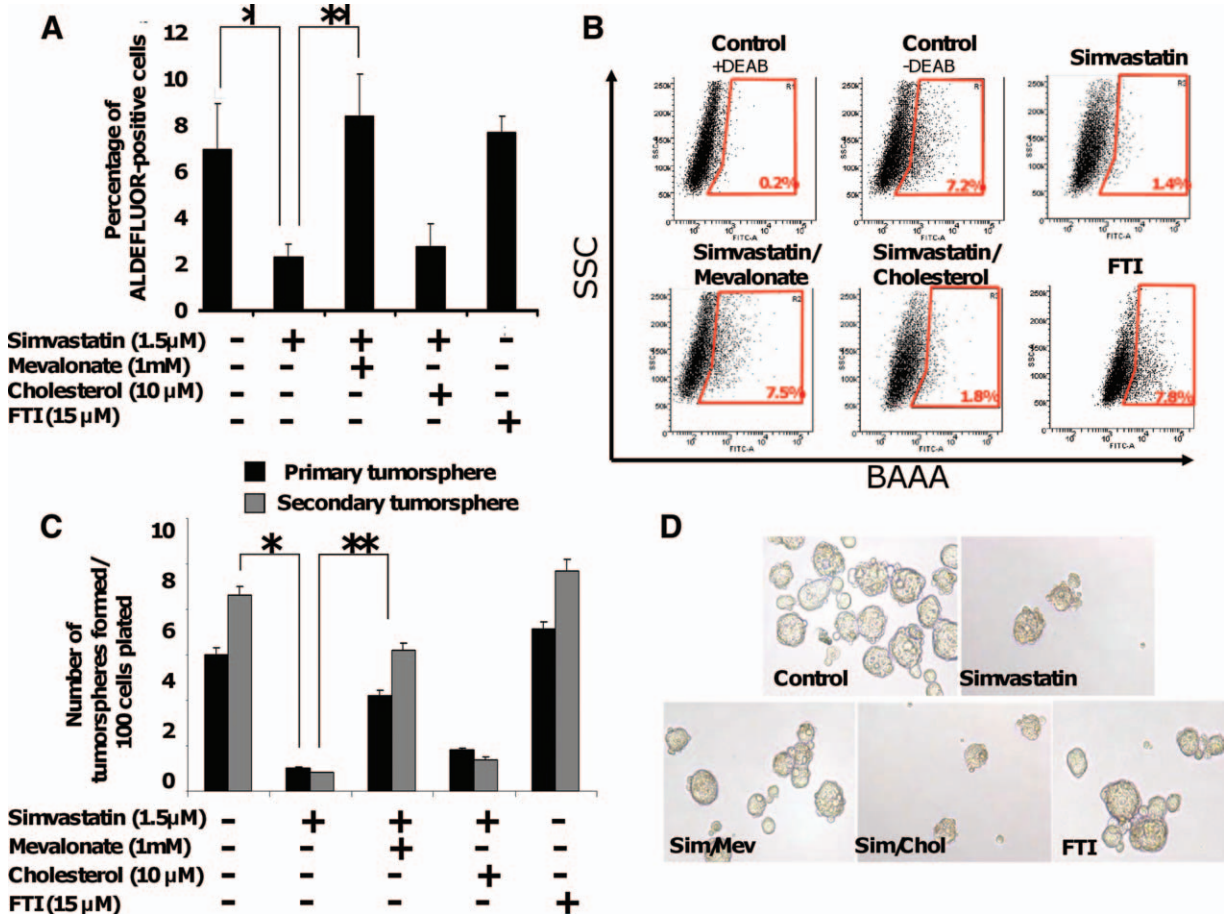

Figure 2. Mevalonic acid (MVA) metabolism blockade reduces the breast cancer stem cell (CSC) populations independently of cholesterol biosynthesis or protein farnesylation. (**A–D**): Simvastatin treatment was used to inhibit MVA metabolism. The effect of Simvastatin on the CSC population was assessed using ALDEFLUOR assay (A, B) and tumorsphere formation (C, D). Simvastatin treatment decreased significantly the ALDEFLUOR-positive population and the primary and secondary tumorsphere formation (*, $p < .01$; Fisher test); MVA rescued the Simavastatin effect (**, $p < .02$; Fisher test), whereas cholesterol did not. Representative flow charts for ALDEFLUOR assay (B) and pictures for primary tumorspheres are represented (D). To test the impact of protein farnesylation in mediating the MVA blockade effect on the CSC population, we treated cells with the FTI (FTI-277). FTI treatment had no effect on the CSC population as assessed by ALDEFLUOR assay or tumorsphere formation. Similar results were observed for each cell line tested (SUM149 shown here; Supporting Information Figs. 5, 6 for SUM159 and HCC1954). Error bars represent mean ± SD. Abbreviations: BAAA, BODIPY aminoacetaldehyde; DEAB, diethylaminobenzaldehyde; FTI, farnesyl transferase inhibitor; SSC, side scatter.

inhibition, we incubated cells with Simvastatin in combination with geranylgeranyl pyrophosphate (GGPP), which serves as a specific isoprenoid substrate for protein GG (Fig. 1B). Exogenous addition of GGPP prevented the Simvastatin-mediated decrease of the CSC population (Fig. 3B; Supporting Information Fig. 6).

The *PGGT1B* gene encodes the beta subunit of the protein GGTase type I (GGTase-I), which catalyzes protein GG. We developed PGGT1B-small interfering RNA (siRNA) constructs to knockdown GGT enzymatic activity. We used three independent PGGT1B-siRNAs that completely abolished PGGT1B protein expression compared with siRNA controls (Fig. 3C; Supporting Information Fig. 7). Knockdown of PGGT1B reduced both the ALDEFLUOR-positive population and the tumorsphere formation ability, thus recapitulating the pharmacological blockade and confirming the specificity of GGTI treatment on the CSC population (Fig. 3D, 3E; Supporting Information Fig. 7). Thus, protein GG inhibition via direct inhibition of GGTase-I mimics MVA metabolism blockade on the CSC component, suggesting that blocking the HMG-CoA/GGPP-dependent pathway may be an appropriate therapeutic approach to target the basal/mesenchymal breast CSC.

MVA Blockade Targets Breast CSC Through RHOA/P27^{kip1} Signaling

A defect in protein GG impairs small GTP-binding proteins, especially RHO family proteins [22]. GG of RHO proteins is necessary for their proper localization to the cell membrane and subsequent functions. RHOA regulates P27^{kip1} by mediating its phosphorylation on Thr187 by CDK2, subsequent translocation of P27 from the nucleus to the cytosol, and enhancing its degradation in the cytoplasm [23, 24]. In the absence of GG, RHOA is unable to carry out these functions and P27^{kip1} accumulates in the nucleus [25]. Because P27^{kip1} is known to regulate stem cell self-renewal [26, 27], we explored the role of RHOA/P27^{kip1} signaling in mediating the effect of GGTI treatment on the CSC population.

We first used a biochemical fractionation method to confirm the subcellular localization of RHOA. Cellular lysates from GGTI-treated SUM159 and control cells were

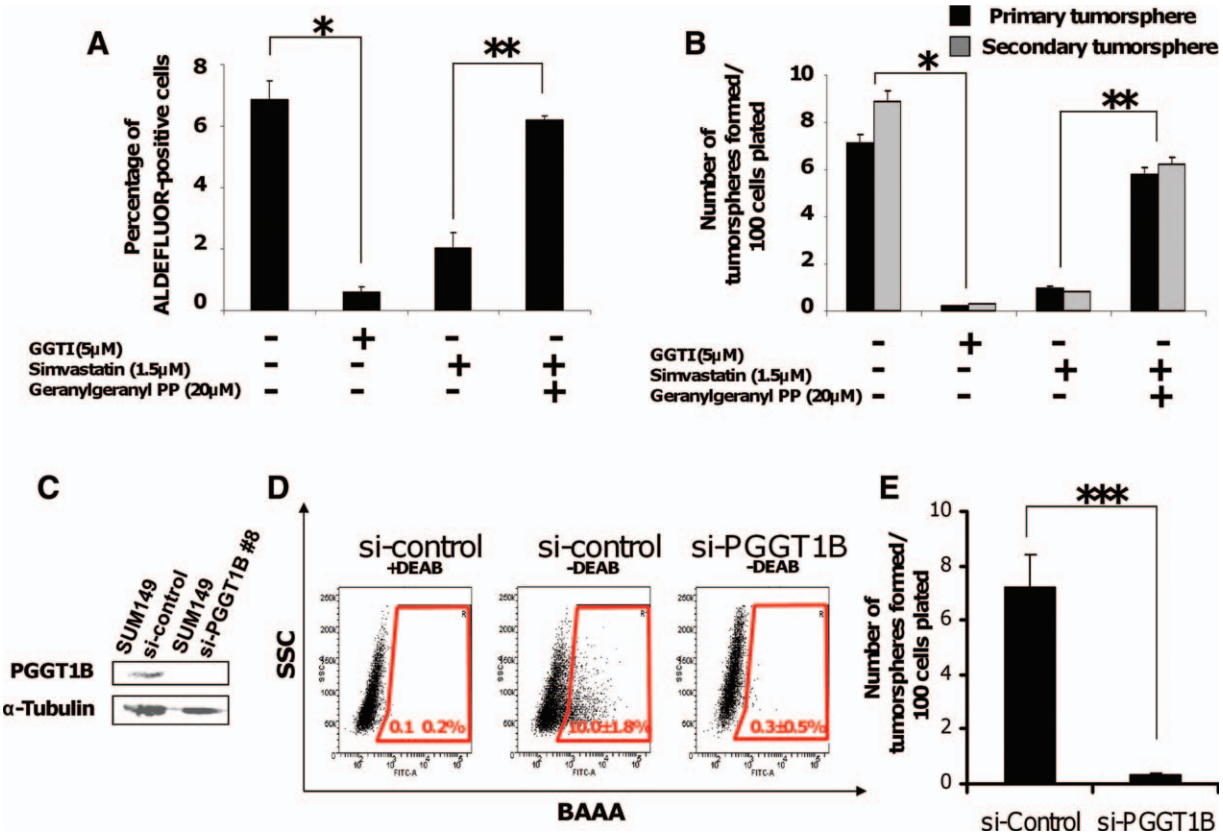

Figure 3. Protein geranylgeranylation (GG) inhibition decreases the breast cancer stem cell (CSC) population. (**A, B**): To evaluate the effect of protein GG inhibition on the breast CSC population, we treated cell lines with the geranylgeranyl transferase inhibitor (GGTI-298) and performed ALDEFLUOR assays (A) and tumorsphere formation assays (B). GGTI treatment drastically decreased the ALDEFLUOR-positive population and the primary and secondary tumorsphere formation (*, $p < .001$; Fisher test). The specific role of protein GG in CSC biology was confirmed by the rescue of Simvastatin treatment effect by geranylgeranyl PP supplementation (**, $p < .01$; Fisher test). (**C, D**): We use an siRNA construct to knock down PGGT1B expression, the gene coding for the beta subunit of protein GGTase type I responsible for protein GG (C). The GGTI effect on the CSC population was recapitulated with depletion of PGGT1B leading to eradication of the ALDEFLUOR-positive population (Fisher test; $p < .001$) (D) and a complete inhibition of tumorsphere formation (**E**) (***, $p < .001$; Fisher test). Similar results were observed for each cell line tested (SUM149 shown here; Supporting Information Figs. 5, 6 for SUM159 and HCC1954). Error bars represent mean ± SD. Abbreviations: BAAA, BODIPY aminoacetaldehyde; DEAB, diethylaminobenzaldehyde; GGTI, geranylgeranyl transferase I; GGPP, geranylgeranyl pyrophosphate.

fractionated into membrane and cytosolic fractions and immunoblotted with anti-RHOA antibody. As expected, we observed that GGTI treatment decreased the amount of RHOA in the membrane fraction, suggesting an inhibition of RHOA function (Fig. 4A).

One mechanism by which GGTIs could suppress CSC self-renewal is through inhibition of RHOA GG and increased $P27^{kip1}$ accumulation, which in turn would result in inhibition of CDK phosphorylation of RB. Therefore, we determined the impact of GGTI treatment and RHOA inactivation by measuring the level of $P27^{kip1}$ and RB protein phosphorylation by Western blotting. After GGTI treatment, we observed an increase of $P27^{kip1}$ protein levels and a decrease of RB phosphorylation (Fig. 4B). The $P27^{kip1}$ protein level increase was associated with nuclear accumulation of this protein after GGTI treatment (Fig. 4C). These results suggest that GGTI-298 inhibition of RHOA GG prevented RHOA from inducing the degradation of $P27^{kip1}$, which in turn resulted in its nucleus accumulation. Moreover cell cycle analysis revealed that GGTI-298 treatment induces an accumulation of cells in G1 phase (Supporting Information Fig. 8). These results confirm that GGTI treatment perturbs the cell cycle progression through a dysregulation of the CCND1/P27/RB1/CCNE signaling.

We next determined whether depletion of $P27^{kip1}$ could rescue breast CSCs from the effects of inhibition of GG and inactivation of RHOA, and whether direct inhibition of RHOA could mimic the effects of GGTIs. To this end, we used both a P27-siRNA and an inhibitor of RHO activity (C3 transferase). P27-siRNA inhibited $P27^{kip1}$ protein expression (Supporting Information Fig. 9) and induced an increase of the CSC population as measured by the ALDEFLUOR-positive population (Fig. 4D). This result shows that P27 negatively regulates breast CSCs and is consistent with previous studies reporting the role of $P27^{kip1}$ in the induction of embryonic and hematopoietic stem cells differentiation [26, 28]. Interestingly, $P27^{kip1}$ knockdown prevented the eradication of the CSC population by the GGTI treatment. The RHO inhibitor decreased the CSC population and induced a nuclear accumulation of $P27^{kip1}$ mimicking the GGTI effect. However, depleting $P27^{kip1}$ prevented the RHO inhibitor from decreasing the CSC population (Fig. 4C, 4D).

These results suggest that the ability of GGTI to inhibit CSC self-renewal requires inactivation of RHOA and increased $P27^{kip1}$ protein levels, and that the pivotal role that $P27^{kip1}$ plays in breast CSC regulation is downstream of protein GG (Fig. 4E).

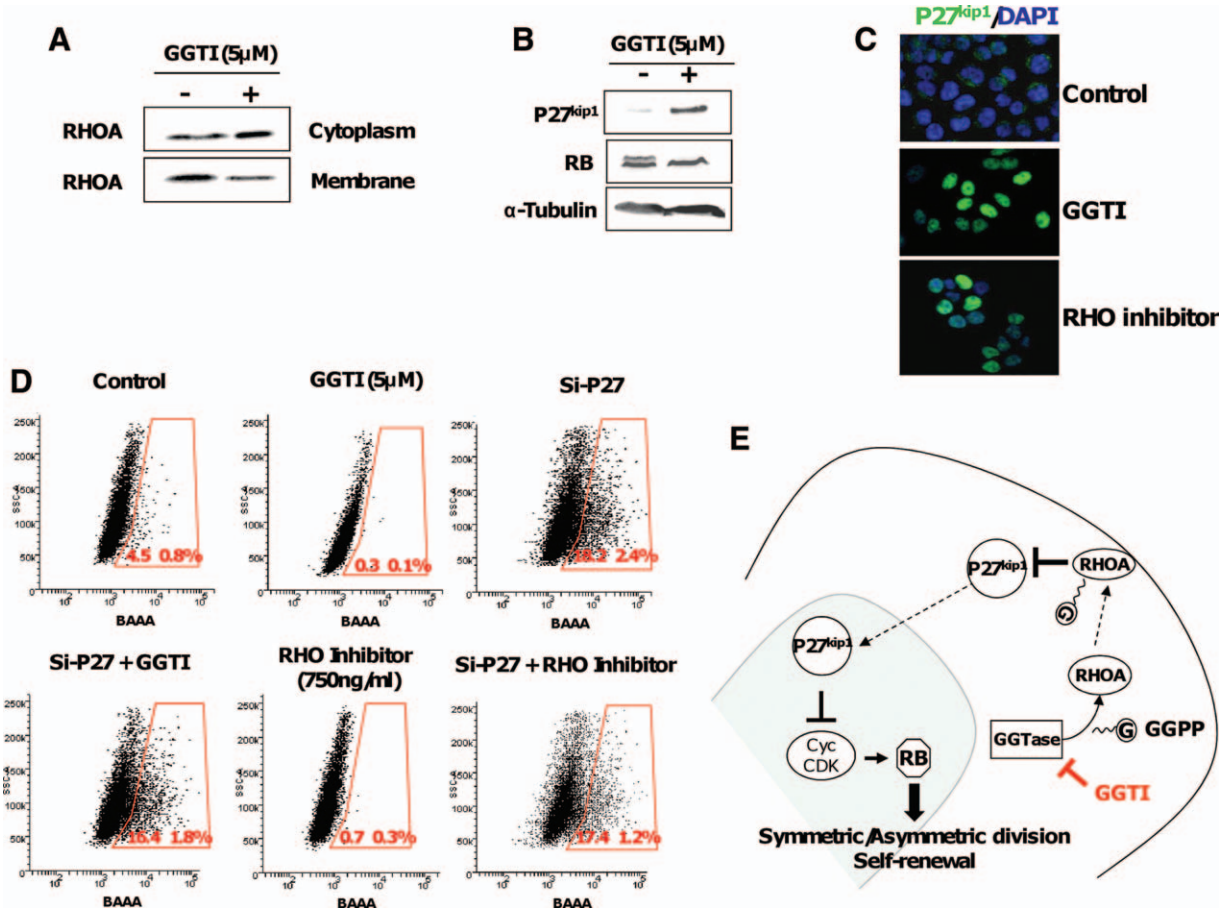

Figure 4. Mevalonic acid (MVA) blockade effect on breast cancer stem cell (CSC) is mediated through RHOA/P27^{kip1} signaling. (**A**): To evaluate the effect of GGTI treatment on RHOA/P27^{kip1} signaling, we performed a biochemical cell fractionation and a Western blot on cytosolic and membrane fractions to determine RHOA protein localization. We observed that GGTI treatment significantly decreased the amounts of RHOA associated with the membrane compared to the nontreated cells (control). (**B**): Using immunoblotting, we observed that GGTI treatment increased P27^{kip1} expression and induced a hypophosphorylation of RB protein. (**C**): Using immunofluorescence staining on GGTI-treated cells, we confirmed that protein GG inhibition induced an increase of P27^{kip1} protein expression (staining in green) that is relocalized in the nucleus (nuclei were counterstained in blue with DAPI). Similarly inhibition of RHOA induced a relocalization of P27^{kip1} protein in the nucleus. (**D**): We measured the effect of P27^{kip1} knockdown and RHOA inhibition on the CSC population using an siRNA construct and a small molecule inhibitor (C3 transferase), respectively. P27^{kip1} knockdown induced an expansion of the ALDEFLUOR-positive cell population that prevented the GGTI effect on the CSC population. RHOA inhibition decreased the ALDEFLUOR-positive population and this effect was rescued by P27^{kip1} knockdown. (**E**): Potential RHOA/P27^{kip1} signaling in CSCs treated with GGTI. RHOA needs to be geranygeranylated to translocate to the membrane and be activated. Activated RHOA protein is known to regulate P27^{kip1} by enhancing its degradation and inhibiting its translocation to the nucleus where it controls cell cycle progression through the "R point". This checkpoint under the control of CCND1/P27^{kip1}/RB/CCNE signaling has been defined as an important cell cycle stage controlling stem cell fate allowing equilibrium between self-renewal and committed cell fate decision. When CSCs are treated with GGTI, RHOA is not activated and P27^{kip1} is translocated to the nucleus where it inhibits RB activation and favors CSC differentiation. Results are represented by mean ± SD. Abbreviations: BAAA, BODIPY aminoacetaldehyde; DAPI, 4′,6-diamidino-2-phenylindole; GGTI, geranylgeranyl transferase I; GGPP, geranylgeranyl pyrophosphate; RHOA, Ras homolog family member A.

GGTI Treatment Reduces the CSC Population in Human Primary Tumor Xenografts

We studied the impact of GGTI treatment on two different primary human breast tumors (T226 and T214). Cells from these tumors were transplanted orthotopically into the humanized cleared fat pads of NOD/SCID mice, without cultivation in vitro. Using these models, we previously demonstrated that the CSC population was exclusively contained in the ALDEFLUOR-positive population [12]. We injected 100,000 cancer cells into the humanized fat pads of NOD/SCID mice and monitored tumor growth. When the tumor size was approximately 150 mm^3, we started the treatment with GGTI (100 mg/kg daily for 2 weeks) and docetaxel (10 mg/kg weekly for 2 weeks) as single agents or in combination. Tumor growth was compared with that of saline-injected controls. We observed an inhibition of the T226 xenograft growth by GGTI, docetaxel, and the combination (Fig. 5A). Docetaxel and GGTI treatment had little effect on the T214 xenograft (Supporting Information Fig. 10). This observation was reminiscent of the T214 patient clinical outcome, who presented a significant chemoresistance to docetaxel.

After 2 weeks of treatment, the animals were sacrificed, and the number of ALDEFLUOR-positive CSCs was measured in each residual tumor (Fig. 5B; Supporting Information Fig. 10). For T226, but not T214, xenograft cancer cells isolated from docetaxel-treated tumors showed a moderate increase in the ALDEFLUOR-positive population compared to the untreated control. This observation is consistent with previous reports that described an enrichment in the CSC population in residual tumors treated with conventional chemotherapy [29,

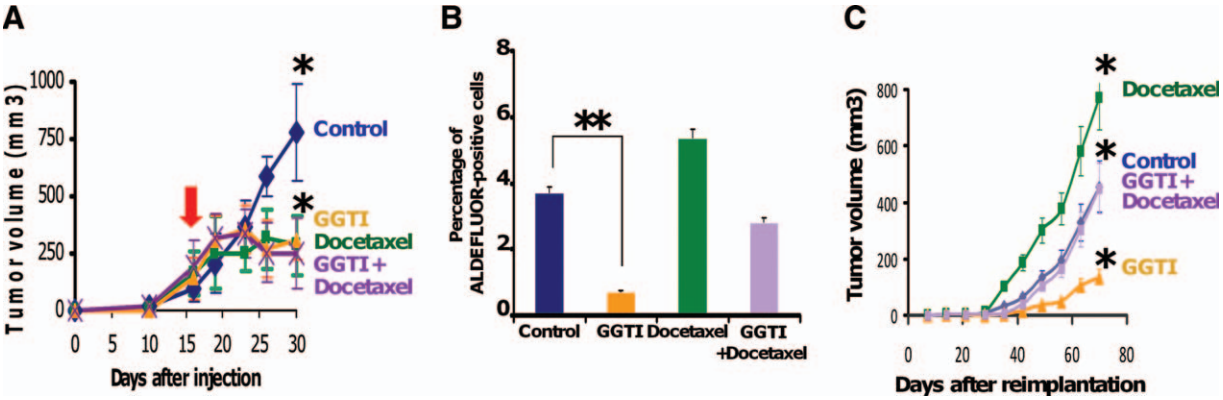

Figure 5. Effect of GGTI treatment on the breast cancer stem cell (CSC) population in vivo. (**A–C**): For each xenograft, 100,000 cells were injected into the mammary fat pad of mice. (A): Tumor size before and during the course of each indicated treatment (arrow indicates beginning of the treatment). Similar results were observed for each sample (T226 shown here; see Supporting Information Fig. 10 for T214), with a statistically significant size reduction of the tumor treated with GGTI alone, with docetaxel alone or in combination compared with the control tumors (*, $p < .03$; *t*-test). (**B, C**): Docetaxel-treated tumors showed similar or an increased percentage of ALDEFLUOR-positive cells compared with the control, whereas GGTI treatment alone produced a statistically significant decrease in ALDEFLUOR-positive cells (**, $p < .01$; Fisher test). GGTI treatment prevented the expansion of CSC induced by docetaxel when both drugs are used in combination (B). (C): About 5,000 cells obtained from these xenografts were implanted in the mammary fat pad of secondary mice, which received no further treatment. Cells from GGTI-treated tumor cells resulted in significant tumor regrowth delay compared to the control, whereas docetaxel-treated tumor cells showed a significant increase in tumor regrowth kinetics (*, $p < .01$; *t*-test). Similarly to our previous results, tumor cells isolated from tumors treated with the combination showed a regrowth capacity comparable to the control. Four mice were injected for each xenotransplant and for each group. Error bars represent mean ± SD. Abbreviation: GGTI, geranylgeranyl transferase I.

30]. In contrast, xenografts treated with GGTI presented a decrease of the ALDEFLUOR-positive population by more than 70% (Fig. 5B). Furthermore, GGTI treatment prevented the expansion of CSC population induced by docetaxel when both drugs were used in combination. These results demonstrate that GGTI treatment specifically targets the CSC population in vivo alone or in combination with chemotherapy.

To functionally prove the reduction of the CSC population in the GGTI-treated tumors, we determined the ability of treated cells to form tumors in vivo by reimplantating cells from treated tumors in secondary mice. Tumorigenicity is directly related to the presence of CSCs and this assay gives an estimate of the proportion of residual tumorigenic CSCs. For each treatment condition (control, GGTI, docetaxel, and combination), 5,000 cells isolated from treated tumors were reimplanted. Tumor cells isolated from GGTI-treated tumors showed a delay in tumor regrowth compared to the cells isolated from control tumors. In sharp contrast, cells isolated from docetaxel-treated tumors showed an increase of tumor regrowth compared to vehicle or GGTI-treated tumors (Fig. 5C; Supporting Information Fig. 10). Cells isolated from tumors treated with the GGTI/docetaxel combination showed a reduced regrowth capacity compared to the docetaxel-treated tumors. These results confirm the ability of the GGTI treatment to target the CSC population in vivo.

Discussion

Targeting breast CSCs for cancer therapy is a promising and developing field. However, to develop an effective anticancer therapeutic strategy it will be necessary to take into account several parameters. One of the challenges is to consider the molecular heterogeneity that may exist between CSCs from different breast cancer molecular subtypes. The tumorigenic potential of CSCs is dependent on the cell of origin (i.e., the targeted CSC) and the nature of the cancer-promoting mutations [10]. Basal and luminal breast cancers display different gene expression profiles that clearly define two distinct (still heterogeneous) entities [9]. These differences may be, at least in part, due to different CSCs regulated by different signaling pathways.

We sought to identify molecular pathways specific for luminal or basal CSCs by using a universal functional assay based on stem cell ability to grow in floating colonies, the tumorspheres. Using gene expression profiling, we were not able to identify specific gene sets differentially expressed in luminal tumorspheres compared to cognate cells cultured in adherent conditions. This result may be explained by the lack of CSC enrichment in luminal tumorspheres compared to adherent cells. Our failure to identify CSC markers in luminal breast tumors shows that the tumorsphere assay is not appropriate for the identification of luminal CSC, and that other strategies must be pursued. A recent study has identified a potential hormone-independent CSC population ($ER^-PR^-CK5^+CD44^+$) in a luminal cell line, raising the possibility that CSCs may drive endocrine resistance in hormone-dependent breast cancers [31]. Moreover, recent data also suggest that the residual breast tumor cell populations surviving after hormone therapy may be enriched in populations of cells with both tumor-initiating and mesenchymal features [32, 33]. Hence, luminal CSC markers may open promising perspectives to override endocrine resistance in luminal breast cancers.

In contrast, our gene expression analysis of basal/mesenchymal tumorspheres revealed an enrichment of genes coding for enzymes involved in the MVA metabolic pathway. Using an in vitro assay, we dissected this metabolic pathway and identified protein GG, but not farnesylation or cholesterol biosynthesis, as a critical activity for basal/mesenchymal breast CSC biology. This is consistent with the observation that protein GG is a regulator of mouse embryonic stem cell (ESC) self-renewal [34]. MVA metabolism blockade impairs ESC self-renewal by modulating RHOA/Rho-associated coiled-coil containing protein kinase (ROCK)-dependent cell signaling. Moreover, lack of mevalonate and of its downstream metabolites, mainly GGPP, induces cell differentiation of normal neurons, oligodendrocytes and astroglia, as well as

neuroblastoma cells [35, 36]. This cell differentiation is mediated through the activation of the peroxisome proliferator-activated receptor gamma (PPAR)γ-phosphatase and tensin homolog (PTEN) cascade and subsequent inhibition of phosphoinositide-3-kinase (PI3K)-AKT signaling. Furthermore, deregulation of MVA metabolism induced by ectopic expression of HMGCR promotes oncogenic transformation of hepatocytes [37]. These data and ours are consistent with a preponderant role of MVA metabolism and particularly protein GG in the regulation of self-renewal in basal/mesenchymal breast CSCs. Interestingly, high mRNA levels of MVA pathway genes correlate with poor prognosis and reduced survival of breast cancer patients [37]. Based on these observations, GGTI treatment appears as a promising anti-CSC therapy. The use of statins, which inhibit MVA metabolism, reduces the risk of breast cancer recurrence [38, 39]. This observation may be linked to the inhibition of CSCs.

GGTI blockade has already been shown to induce a significant inhibition of development of a variety of hematopoietic and solid tumors. Conditional knockout mice for *Pggt1b*, the gene encoding GGTase-I, develop significantly less KRAS-induced lung tumors and myeloproliferative neoplasms [40]. Furthermore, GGTI treatment inhibits the growth of human breast cancer xenografts and induces regression of mammary tumors in transgenic mice [25, 41]. Here, we have shown that MVA metabolism blockade through GG inhibition targets breast CSCs in vivo. We compared the effects of the cytotoxic agent docetaxel with those of GGTI on the CSC compartment and on tumor growth in NOD/SCID mice. We assessed the CSC populations by the ALDEFLUOR assay and by serial transplantations in NOD/SCID mice. Using these assays, we determined that chemotherapy treatment alone resulted in a relative increase in the CSC populations. In contrast, GGTI treatment alone or in combination with chemotherapy reduced the CSC population. This is an important observation that warrants further validation in the clinic.

Our results suggest that GGTI treatment may be a new therapeutic approach to target specifically the basal/mesenchymal breast CSC population. However, further studies will be needed to elucidate the complex molecular signaling pathways that link CSC self-renewal to MVA metabolism. One possibility is the inhibition of RHOA function that results in the accumulation of $P27^{kip1}$ in the nucleus after GGTI treatment. The progression in the cell cycle during the G1 phase is under the control of the CCND1/P27/RB1/CCNE signaling. This checkpoint, also called R point, has been defined as an important cell cycle stage controlling stem cell fate allowing equilibrium between self-renewal and committed cell fate decision [27]. Thus, $P27^{kip1}$ deregulation induced by GGTI treatment may modify the G1 phase of the cell cycle, disturb breast CSC self-renewal, and induce differentiation. In support of this hypothesis, knockin mice in which the P27 protein is unable to interact with cyclins and CDKs developed tumors in multiple organs and this high incidence of spontaneous tumors was associated with amplification of stem/progenitor cell populations [42].

Conclusion

Targeting a specific metabolic pathway essential to CSC is a new and promising approach. Several studies have described an association between metabolism and CSC biology, but no therapy has ever been proposed so far. For example, the production of reactive oxygen species (ROS) has been implicated in the regulation of leukemic stem cells and breast CSCs, with a lower ROS concentration in CSCs compared to mature cancer cells [43, 44]. Lower ROS levels in CSCs are associated with increased expression of free radical scavenging systems, which may contribute to tumor radioresistance. We have here demonstrated the role of protein GG in the regulation of breast CSCs. Clinical phase I studies using GGTI have demonstrated a lack of toxicity [45]. This suggests that interfering with protein GG may be a novel strategy to target breast CSCs in humans. Because these cells may drive tumor progression, metastasis, and chemoresistance, and radioresistance, such strategies may lead to improving outcome for women with breast cancer, not curable with surgery alone.

Acknowledgments

We thank T.T. Nguyen and J. Bonensea for help in the initial phases of the study. We also thank the Association pour la Recherche contre le Cancer for supporting our acquisition of a cell sorter. This study was supported by Inserm, Institut Paoli-Calmettes and grants from the Ligue National Contre le Cancer (Label DB) and Institut National du Cancer (R. Translationnelle 2009, PL Xenotek). F.M. and G.L. have been supported by a fellowship from the Ministry of Research, Association pour la Recherche contre le Cancer, and Institut National du Cancer.

Disclosure of Potential Conflicts of Interest

The authors declare that no potential conflicts of interest exist in this study.

References

1 Wicha MS, Liu S, Dontu G. Cancer stem cells: An old idea—A paradigm shift. Cancer Res 2006;66:1883–1890.
2 Visvader JE, Lindeman GJ. Cancer stem cells in solid tumours: Accumulating evidence and unresolved questions. Nat Rev Cancer 2008;8:755–768.
3 Liu S, Wicha MS. Targeting breast cancer stem cells. J Clin Oncol 2010;28:4006–4012.
4 Charafe-Jauffret E, Ginestier C, Iovino F et al. Breast cancer cell lines contain functional cancer stem cells with metastatic capacity and a distinct molecular signature. Cancer Res 2009;69:1302–1313.
5 Charafe-Jauffret E, Ginestier C, Iovino F et al. Aldehyde dehydrogenase 1-positive cancer stem cells mediate metastasis and poor clinical outcome in inflammatory breast cancer. Clin Cancer Res 2010;16:45–55.
6 Liu H, Patel MR, Prescher JA et al. Cancer stem cells from human breast tumors are involved in spontaneous metastases in orthotopic mouse models. Proc Natl Acad Sci USA 2010;107:18115–18120.
7 Ginestier C, Charafe-Jauffret E, Birnbaum D. Targeting breast cancer stem cells: Fishing season open! Breast Cancer Res 2010;12:312.
8 Ginestier C, Liu S, Diebel ME et al. CXCR1 blockade selectively targets human breast cancer stem cells in vitro and in xenografts. J Clin Invest 2010;120:485–497.
9 Bertucci F, Finetti P, Cervera N et al. How different are luminal A and basal breast cancers? Int J Cancer 2009;124:1338–1348.
10 Visvader JE. Cells of origin in cancer. Nature 2011;469:314–322.
11 Al-Hajj M, Wicha MS, Benito-Hernandez A et al. Prospective identification of tumorigenic breast cancer cells. Proc Natl Acad Sci USA 2003;100:3983–3988.

12 Ginestier C, Hur MH, Charafe-Jauffret E et al. ALDH1 is a marker of normal and malignant human mammary stem cells and a predictor of poor clinical outcome. Cell Stem Cell 2007;1:555–567.
13 Fillmore CM, Kuperwasser C. Human breast cancer cell lines contain stem-like cells that self-renew, give rise to phenotypically diverse progeny and survive chemotherapy. Breast Cancer Res 2008;10:R25.
14 Honeth G, Bendahl PO, Ringner M et al. The CD44+/. Breast Cancer Res 2008;10:R53.
15 Dontu G, Abdallah WM, Foley JM et al. In vitro propagation and transcriptional profiling of human mammary stem/progenitor cells. Genes Dev 2003;17:1253–1270.
16 Ponti D, Costa A, Zaffaroni N et al. Isolation and in vitro propagation of tumorigenic breast cancer cells with stem/progenitor cell properties. Cancer Res 2005;65:5506–5511.
17 Xiao Y, Ye Y, Yearsley K et al. The lymphovascular embolus of inflammatory breast cancer expresses a stem cell-like phenotype. Am J Pathol 2008;173:561–574.
18 Subramanian A, Tamayo P, Mootha VK et al. Gene set enrichment analysis: A knowledge-based approach for interpreting genome-wide expression profiles. Proc Natl Acad Sci USA 2005;102:15545–15550.
19 Kok M, Koornstra RH, Margarido TC et al. Mammosphere-derived gene set predicts outcome in patients with ER-positive breast cancer. J Pathol 2009;218:316–326.
20 Cheadle C, Watkins T, Fan J et al. GSMA: Gene Set Matrix Analysis, An automated method for rapid hypothesis testing of gene expression data. Bioinform Biol Insights 2009;1:49–62.
21 Goldstein JL, Brown MS. Regulation of the mevalonate pathway. Nature 1990;343:425–430.
22 Casey PJ. Mechanisms of protein prenylation and role in G protein function. Biochem Soc Trans 1995;23:161–166.
23 Hirai A, Nakamura S, Noguchi Y et al. Geranylgeranylated rho small GTPase (s) are essential for the degradation of p27Kip1 and facilitate the progression from G1 to S phase in growth-stimulated rat FRTL-5 cells. J Biol Chem 1997;272:13–16.
24 Hu W, Bellone CJ, Baldassare JJ. RhoA stimulates p27(Kip) degradation through its regulation of cyclin E/CDK2 activity. J Biol Chem 1999;274:3396–3401.
25 Kazi A, Carie A, Blaskovich MA et al. Blockade of protein geranylgeranylation inhibits Cdk2-dependent p27Kip1 phosphorylation on Thr187 and accumulates p27Kip1 in the nucleus: implications for breast cancer therapy. Mol Cell Biol 2009;29:2254–2263.
26 Menchon C, Edel MJ, Izpisua Belmonte JC. The cell cycle inhibitor p27 (Kip1) controls self-renewal and pluripotency of human embryonic stem cells by regulating the cell cycle, Brachyury And Twist. Cell Cycle 2011;10:1435–1447.
27 Orford KW, Scadden DT. Deconstructing stem cell self-renewal: Genetic insights into cell-cycle regulation. Nat Rev Genet 2008;9:115–128.
28 Walkley CR, Fero ML, Chien WM et al. Negative cell-cycle regulators cooperatively control self-renewal and differentiation of haematopoietic stem cells. Nat Cell Biol 2005;7:172–178.
29 Lee HE, Kim JH, Kim YJ et al. An increase in cancer stem cell population after primary systemic therapy is a poor prognostic factor in breast cancer. Br J Cancer 2001;104:1730–1738.
30 Li X, Lewis MT, Huang J et al. Intrinsic resistance of tumorigenic breast cancer cells to chemotherapy. J Natl Cancer Inst 2008;100: 672–679.
31 Horwitz KB, Dye WW, Harrell JC et al. Rare steroid receptor-negative basal-like tumorigenic cells in luminal subtype human breast cancer xenografts. Proc Natl Acad Sci USA 2008;105:5774–5779.
32 Creighton CJ, Li X, Landis M et al. Residual breast cancers after conventional therapy display mesenchymal as well as tumor-initiating features. Proc Natl Acad Sci USA 2009;106:13820–13825.
33 Haughian JM, Pinto MP, Harrell JC et al. Maintenance of hormone responsiveness in luminal breast cancers by suppression of Notch. Proc Natl Acad Sci USA 2012;109:2742–2747.
34 Lee MH, Cho YS, Han YM. Simvastatin suppresses self-renewal of mouse embryonic stem cells by inhibiting RhoA geranylgeranylation. Stem Cells 2007;25:1654–1663.
35 Marz P, Otten U, Miserez AR. Statins induce differentiation and cell death in neurons and astroglia. Glia 2007;55:1–12.
36 Paintlia AS, Paintlia MK, Singh AK et al. Activation of PPAR-gamma and PTEN cascade participates in lovastatin-mediated accelerated differentiation of oligodendrocyte progenitor cells. Glia 2010;58: 1669–1685.
37 Clendening JW, Pandyra A, Boutros PC et al. Dysregulation of the mevalonate pathway promotes transformation. Proc Natl Acad Sci USA 2010;107:15051–15056.
38 Ahern TP, Pedersen L, Tarp M et al. Statin prescriptions and breast cancer recurrence risk: a Danish nationwide prospective cohort study. J Natl Cancer Inst 2011;103:1461–1468.
39 Chae YK, Valsecchi ME, Kim J et al. Reduced risk of breast cancer recurrence in patients using ACE inhibitors, ARBs, and/or Statins. Cancer Invest 2011;29:585–593.
40 Sjogren AK, Andersson KM, Khan O et al. Inactivating GGTase-I reduces disease phenotypes in a mouse model of K-RAS-induced myeloproliferative disease. Leukemia 2011;25:186–189.
41 Sun J, Ohkanda J, Coppola D et al. Geranylgeranyltransferase I inhibitor GGTI-2154 induces breast carcinoma apoptosis and tumor regression in H-Ras transgenic mice. Cancer Res 2003;63: 8922–8929.
42 Besson A, Hwang HC, Cicero S et al. Discovery of an oncogenic activity in p27Kip1 that causes stem cell expansion and a multiple tumor phenotype. Genes Dev 2007;21:1731–1746.
43 Abdel-Wahab O, Levine RL. Metabolism and the leukemic stem cell. J Exp Med 2010;207:677–680.
44 Diehn M, Cho RW, Lobo NA et al. Association of reactive oxygen species levels and radioresistance in cancer stem cells. Nature 2009; 458:780–783.
45 O'Dwyer PJ, Gallagher M, Nguyen B et al. Phase I accelerated dose-escalating safety and pharmacokinetic (PK) study of GGTI-2418, a novel geranylgeranyl transferase I inhibitor in patients with refractory solid tumors. Poster presented at: The 8th International Symposium on Targeted Anticancer Therapies; 2010; North Bethesda, MD.
46 Charafe-Jauffret E, Ginestier C, Monville F et al. Gene expression profiling of breast cell lines identifies potential new basal markers. Oncogene 2006;25:2273–2284.
47 Irizarry RA, Hobbs B, Collin F et al. Exploration, normalization, and summaries of high density oligonucleotide array probe level data. Biostatistics 2003;4:249–264.
48 Mootha VK, Lindgren CM, Eriksson KF et al. PGC-1alpha-responsive genes involved in oxidative phosphorylation are coordinately downregulated in human diabetes. Nat Genet 2003;34:267–273.
49 Kim SY, Volsky DJ. PAGE: parametric analysis of gene set enrichment. BMC Bioinformatics 2005;6:144.
50 Eisen MB, Spellman PT, Brown PO et al. Cluster analysis and display of genome-wide expression patterns. Proc Natl Acad Sci USA 1998; 95:14863–14868.

See www.StemCells.com for supporting information available online.